Electronic Supplementary Information

1. Experimental Methods

The measurements were performed at beamline ID26[1,2] of the European Synchrotron (ESRF) in Grenoble. The incident energy was selected using the <111> reflection from a double Si crystal monochromator. Rejection of higher harmonics was achieved by three Si mirrors at an angles of 3.0, 3.5 and 4.0 mrad relative to the incident beam. Resonant inelastic X-ray scattering (RIXS) at the U M_5 edge was measured by scanning the emission energy at the fixed incident energy using an X-ray emission spectrometer. The position of the elastic peak was calibrated by measuring the elastic scattering from the Lead tape. The sample, analyzer crystal and photon detector (silicon drift diode) were arranged in a vertical Rowland geometry. The emission energy was selected using the <220> reflection of five spherically bent Si crystal analyzers (with 1m bending radius) aligned at the 65° Bragg angle. The paths of the incident and emitted X-rays through air were minimized in order to avoid losses in intensity due to absorption. The intensity was normalised to the incident flux. A combined (incident convoluted with emitted) energy resolution of 1.0 eV was obtained as determined by measuring the full width at half maximum (FWHM) of the elastic peak.

All samples were prepared from depleted nuclear grade UO_{2+x}, supplied by FBFC International (Dessel, Belgium). An assessment of the impurity content of this powder has been reported elsewhere.[3] Conditions for preparation of the various samples were evaluated via simultaneous thermal analysis (Netzsch STA 449 F1 Jupiter). The preparation of $UO_{2.0}$, U_4O_9, and U_3O_7 has been described in detail in Refs. 4 and 5[4,5]. U_3O_8 powder was synthesized by oxidation of as-received UO_{2+x} powder at 500°C or 4 h under a constant flow of dry air (N_2 / 21 vol.% O_2). A wet - chemical route was employed to produce β-UO_3. As-received UO_{2+x} powder was first dissolved in nitric acid and subsequently titrated with an excess of an ammonia aqueous solution, which results in precipitation of ammonium diuranate (ADU). β-UO_3 was then obtained by calcining the ADU powder at 550°C for 30 min. Phase purity of all samples was confirmed via X - ray diffraction. Powders (30-50 mg) were intimately mixed with boron nitride powder and compacted into thin pellets. These pellets were placed in sample holders dedicated to cryostat operation at beamline ID26 and sealed with Kapton foil.

2. Theoretical Calculations

Valence band RIXS calculations at the U M_5 edge were performed by inserting the U 5f and O 2p density of states into the Kramers-Heisenberg equation[6]:

$$F(\Omega,\omega) = \int_{\varepsilon} d\varepsilon \frac{\rho(\varepsilon)\rho'(\varepsilon+\Omega-\omega)}{(\varepsilon-\omega)^2 + \frac{\Gamma_n^2}{4}} \qquad (1)$$

Where p and p' are the density of occupied and unoccupied U f and O p states, while Ω and ω represent the energies of the incident and scattered photons, respectively. Γ_n represents

the lifetime broadening of the U 3d state, which is 3.8 eV[7]. The validity of this approximation has been already evaluated previously by comparison between experimental and theoretical results[8–12].

3. Computed density of states

The calculations were performed using DFT-based Quantum-ESPRESSO simulations package[13]. The computational setup resembles the one used by Beridze and Kowalski[14]. We applied the plane-wave cut off of 50 Ryd and ultra soft pseudopotentials to mimic the presence of core-electrons[15]. In order to capture correctly the strongly correlated *f* electrons, following our previous studies of Uranium-bearing systems[14], we applied the DFT+*U* method[16–18]. We have used the PBEsol exchange-correlation functional[19]. This is because it represents a small modification of the widely used PBE exchange-correlation functional[20], which better reproduces the slowly varying electronic density limit. It results in much better predictions of structural parameters, which is important for the purpose of our research. Nevertheless, there is no significant difference in the performance of the two mentioned functionals for computation of the electronic structures of uranium oxides[14].

For the computation of DOSs we used two approaches. In the first we have applied the standard approach assuming the standard values used in computation of Uranium-systems (U=4.5eV and J=0.54eV)[16] (named **M1).** In addition we computed the Hubbard *U* parameters values using the linear response method of Cococcion & Gironcoli[18]. Here, for the purpose of calculations of the Hubbard correction we represent f orbitals for projection of occupations with the atomic orbitals (**M2**) and the Wannier functions (**M3**).

The initial atomic structures of the simulated oxides came from UO_2[21], β-UO_3[22], U_3O_8[23] and U_3O_7[24] . We have applied the Methfessel−Paxton k-points grids[25]: 4x4x4 for UO_2, 2x2x6 for UO_3 and 3x2x5 for U_3O_8. U_3O_7 has been modelled by a large supercell containing 200 atoms and have been computed on the gamma point only. The lattice parameters have been optimized to the equilibrium values assuming P=0 GPa with the tolerance of 0.1 GPa. The equilibrium was reached assuming the maximal residual force acting on atoms being smaller than 0.005 eV/Å.

Computation of the electronic structure of uranium-oxides is not a trivial task and can often lead to the convergence to a metastate[26]. In order to obtain the correct electronic structure of the considered oxides, for an initial electronic state we computed the expected charges of the different uranium atoms in the considered mixed oxides using bond valence sum (BVS) method[27]. The BVS of U atoms for the considered oxides: U_3O_7 ($\boldsymbol{P}4_2/\mathrm{nZ}(86)$), U_3O_8 ($\boldsymbol{A}\mathrm{mm2}$), UO_3 ($\boldsymbol{P}1211$), and UO_2 ($\boldsymbol{F}\mathrm{m\text{-}3m}$) were calculated and analyzed applying the following formula:

$$V = \sum_i \exp[(R_i - d_i)/b]$$

Here the bond valence parameter R_i and constant *b* are taken from Ref[28]. V and d_i are the corresponding valence and bond lengths for each phase. The BVS results of U atom for the title phases are given in **Table 1** and for the U_3O_7 phase illustrated in Figure 5. The obtained ab-initio charges for U3O8 are (VI) and (V) for U(1) and U(2), respectively. The DFT+U

calculations predicted the AFM state for UO_2 and U_3O_8 and these were used in the analysis. For the more complex structure of U_3O_7 the ground state was calculated to be ferromagnetic.

Table 1. Results of bond valence calculation for U_3O_8 (***A***mm2), UO_3 (***P***1211), and UO_2 (***F***m-3m), respectively.

Phases		U–O bond lengths							Valence Sum (v.u.)
U_3O_8 (*A*mm2)	U(1)	2.074× 2↓	2.445	2.183× 2↓	2.2494× 2↓				5.41
	U(2)	2.074× 2↓	2.2068	2.1214	2.7141	2.1586	2.197		5.61
UO_3 (*P*1211)	U(1)	2.0711	2.2061	2.3904	2.3697	2.3993	1.7391	2.2179	6.35
	U(2)	2.7234	2.3959	2.4926	2.3105	2.4174	1.6959	2.1006	5.76
	U(3)	2.1701	1.7924	2.1694	1.9792	2.086	1.8877		7.94
	U(4)	2.2388	2.1968	2.6891	2.6015	1.5137	2.637	1.6586	10.42
	U(5)	2.7433	2.1142	2.2764	2.4576	2.7672	2.2749	1.6629	6.03
UO_2 (*F*m-3m)	U(1)	2.3677	2.3677	2.3677	2.3677	2.3677	2.3677	2.3677	4.01

Figure 1 - 4 shows partial Density of States (DOS) obtained by different theoretical methods.

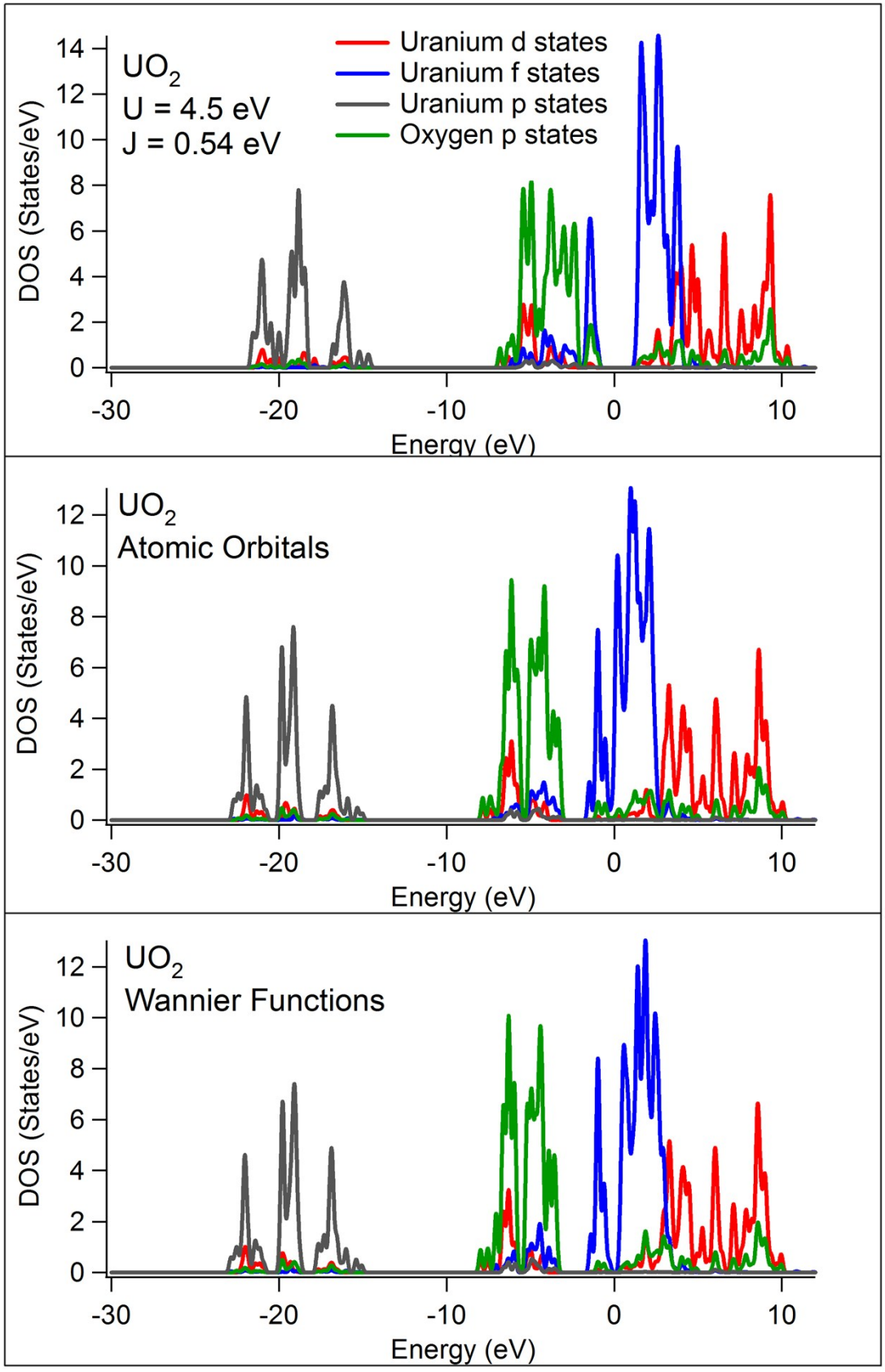

Figure 1. Density of states curves for UO_2

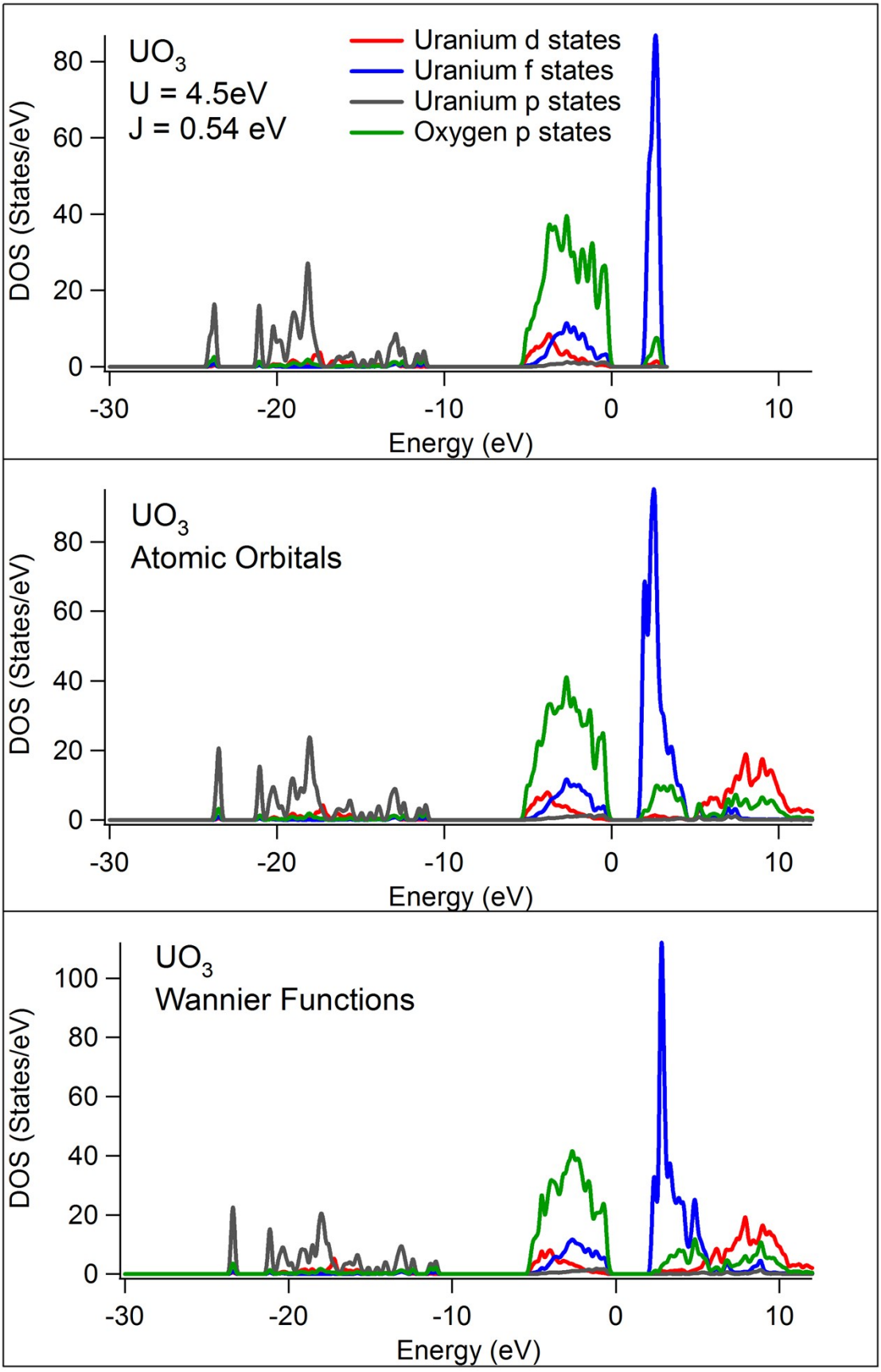

Figure 2. Density of states curves for β-UO_3

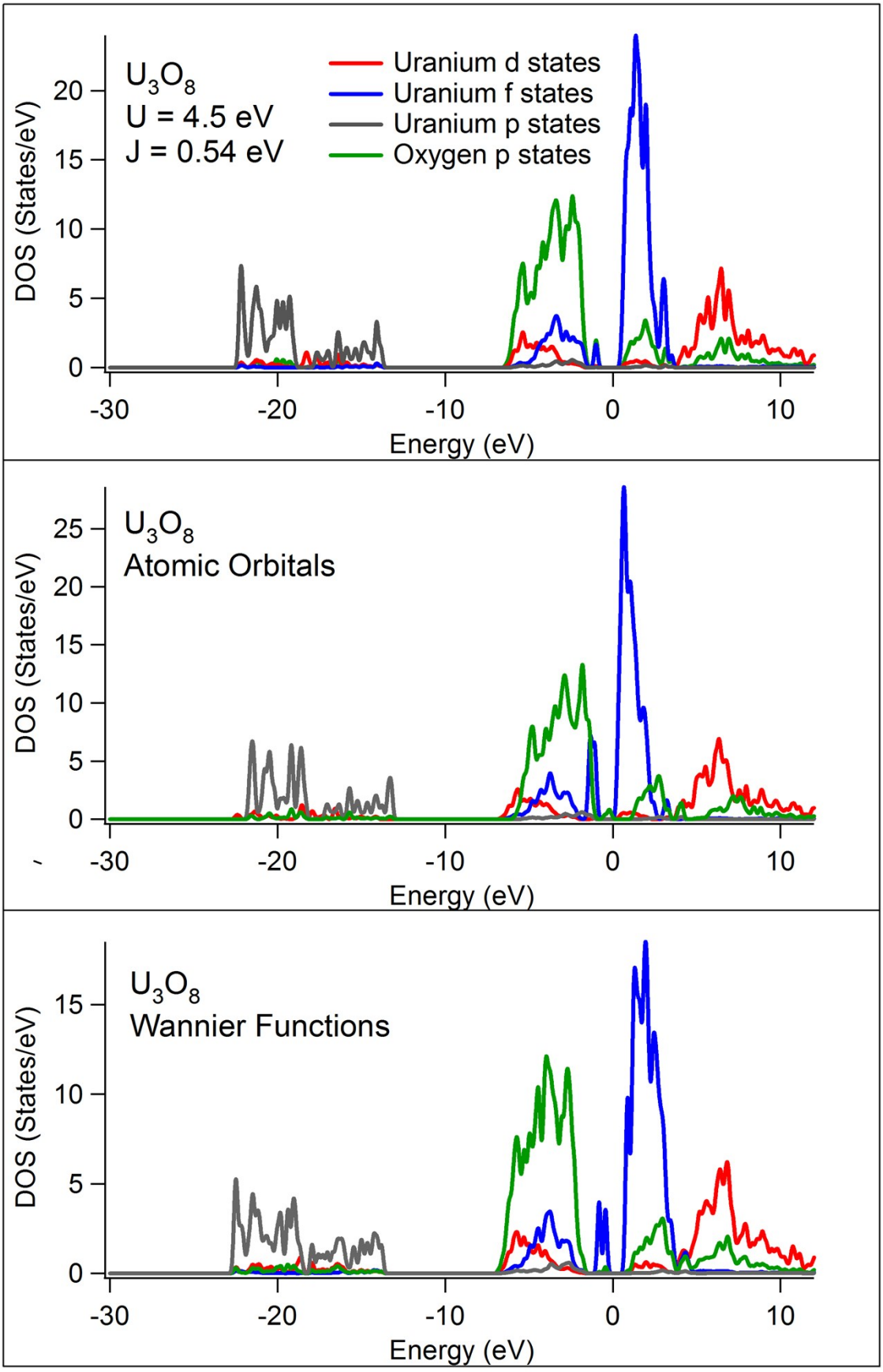

Figure 3. Density of states curves for U_3O_8

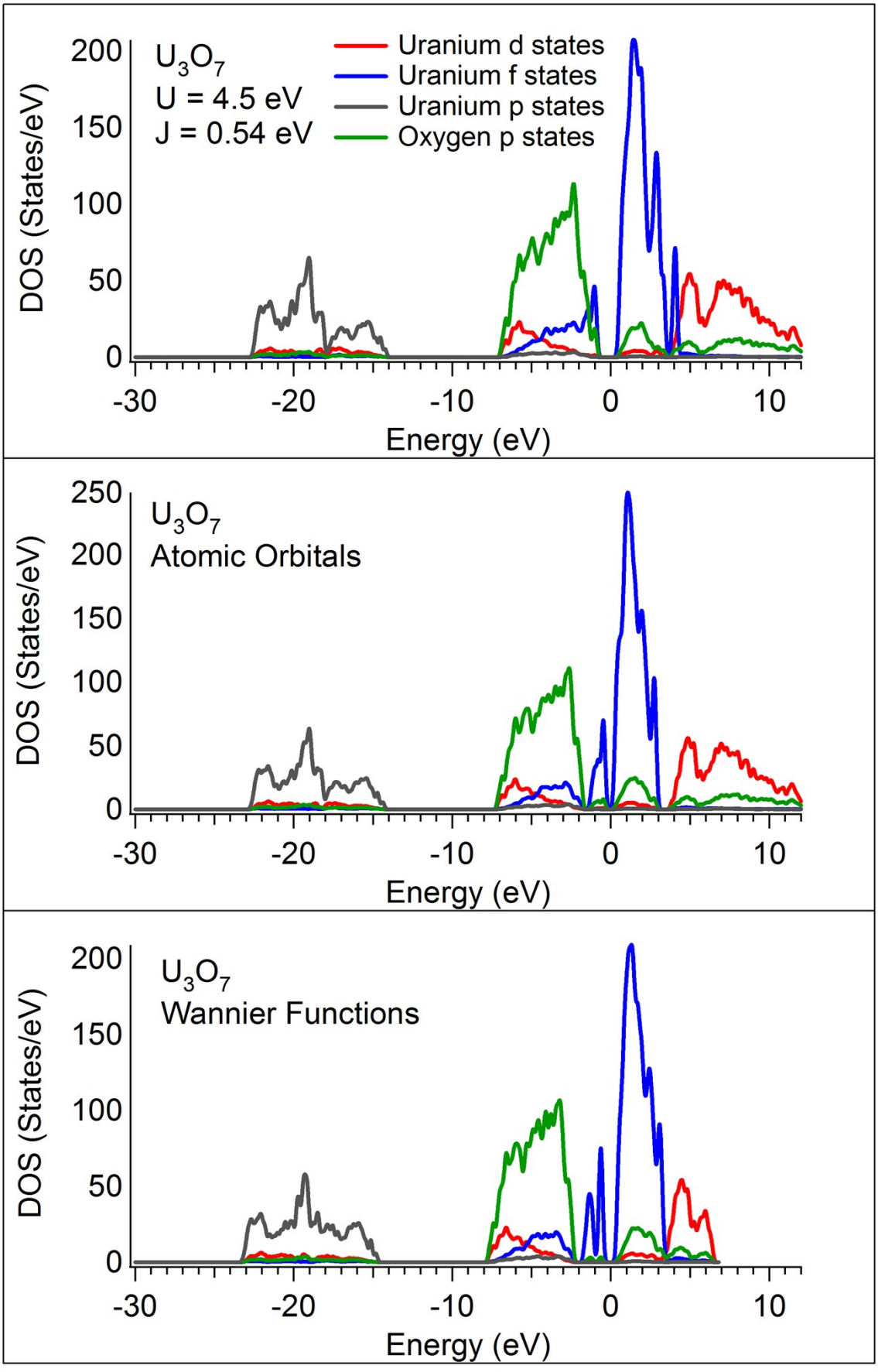

Figure 4. Density of states curves for U_3O_7

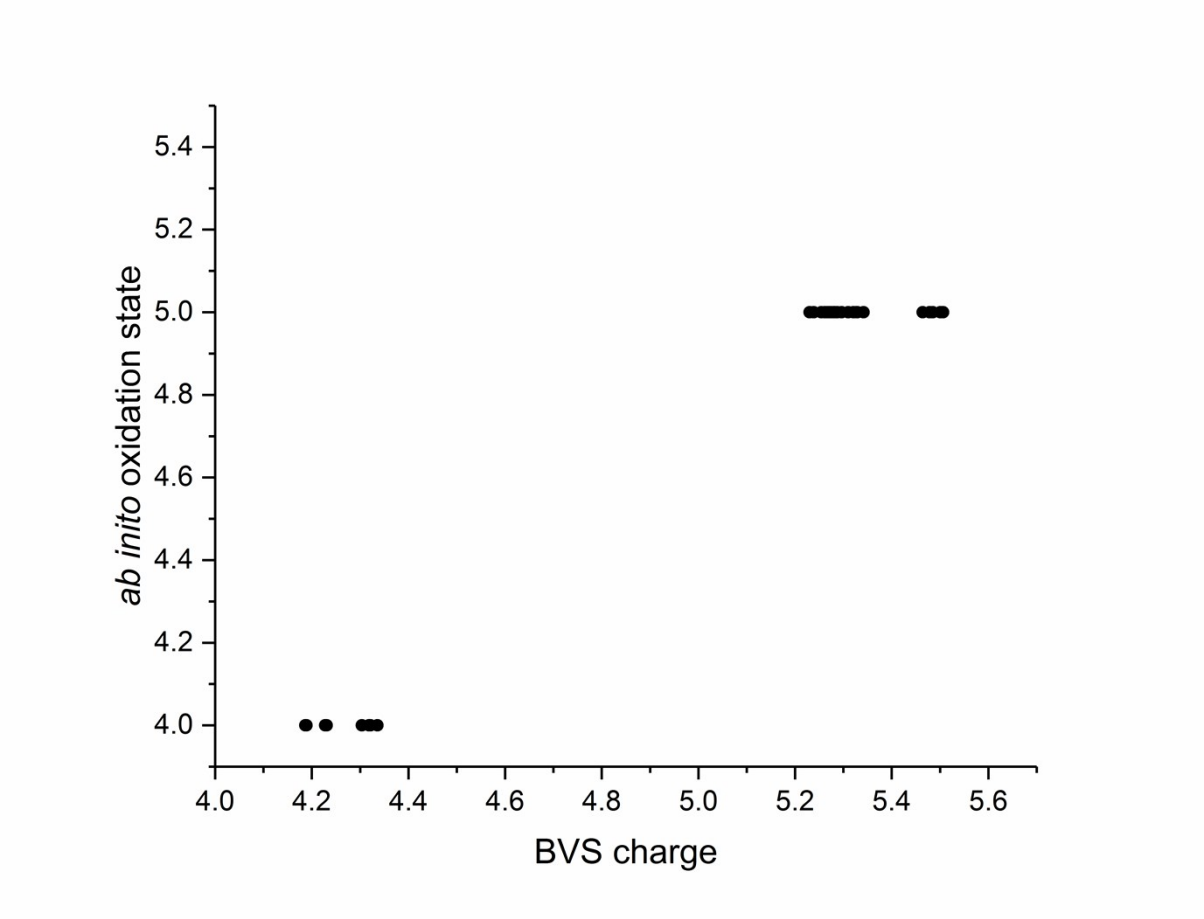

Figure 5. The DFT+U and BVS charges on U atoms in U_3O_7 structure[5].

References:

1 C. Gauthier, V. A. Solé, R. Signorato, J. Goulon and E. Moguiline, *J. Synchrotron Radiat.*, 1999, **6**, 164–6.

2 R. Signorato, V. a Solé and C. Gauthier, *J. Synchrotron Radiat.*, 1999, **6**, 176–8.

3 G. Leinders, T. Cardinaels, K. Binnemans and M. Verwerft, *J. Nucl. Mater.*, 2015, **459**, 135–142.

4 G. Leinders, J. Pakarinen, R. Delville, T. Cardinaels, K. Binnemans and M. Verwerft, *Inorg. Chem.*, 2016, **55**, 3915–3927.

5 G. Leinders, R. Delville, J. Pakarinen, T. Cardinaels, K. Binnemans and M. Verwerft, *Inorg. Chem.*, 2016, **55**, 9923–9936.

6 J. Jiménez-Mier, J. van Ek, D. L. Ederer, T. A. Callcott, J. J. Jia, J. Carlisle, L. Terminello, A. Asfaw and R. C. Perera, *Phys. Rev. B*, 1999, **59**, 2649–2658.

7 M. O. Krause and J. H. Oliver, *J. Phys. Chem. Ref. Data*, 1979, **8**, 329.

8 P. Glatzel, J. Singh, K. O. Kvashnina and J. a van Bokhoven, *J. Am. Chem. Soc.*, 2010, **132**, 2555–7.

9 K. O. Kvashnina, Y. O. Kvashnin and S. M. Butorin, *J. Electron Spectros. Relat. Phenomena*, 2014, **194**, 27–36.

10 K. O. Kvashnina, Y. O. Kvashnin, J. R. Vegelius, A. Bosak, P. M. Martin and S. M. Butorin, *Anal. Chem.*, 2015, **87**, 8772–8780.

11 K. O. Kvashnina, H. C. Walker, N. Magnani, G. H. Lander and R. Caciuffo, *Phys. Rev. B*, 2017, **95**, 245103.

12 J. R. Vegelius, K. O. Kvashnina, M. Klintenberg, I. L. Soroka and S. M. Butorin, *J. Anal. At. Spectrom.*, , DOI:10.1039/c2ja30095h.

13 P. Giannozzi, S. Baroni, N. Bonini, M. Calandra, R. Car, C. Cavazzoni, D. Ceresoli, G. L. Chiarotti, M. Cococcioni, I. Dabo, A. Dal Corso, S. de Gironcoli, S. Fabris, G. Fratesi, R. Gebauer, U. Gerstmann, C. Gougoussis, A. Kokalj, M. Lazzeri, L. Martin-Samos, N. Marzari, F. Mauri, R. Mazzarello, S. Paolini, A. Pasquarello, L. Paulatto, C. Sbraccia, S. Scandolo, G. Sclauzero, A. P. Seitsonen, A. Smogunov, P. Umari and R. M. Wentzcovitch, *J. Phys. Condens. Matter*, 2009, **21**, 395502.

14 G. Beridze and P. M. Kowalski, *J. Phys. Chem. A*, 2014, **118**, 11797–11810.

15 D. Vanderbilt, *Phys. Rev. B*, 1990, **41**, 7892–7895.

16 X.-D. Wen, R. L. Martin, T. M. Henderson and G. E. Scuseria, *Chem. Rev.*, 2013, **113**, 1063–1096.

17 B. Himmetoglu, A. Floris, S. de Gironcoli and M. Cococcioni, *Int. J. Quantum Chem.*, 2014, **114**, 14–49.

18 M. Cococcioni and S. de Gironcoli, *Phys. Rev. B*, 2005, **71**, 35105.

19 J. P. Perdew, A. Ruzsinszky, G. I. Csonka, O. A. Vydrov, G. E. Scuseria, L. A. Constantin, X. Zhou and K. Burke, *Phys. Rev. Lett.*, 2008, **100**, 136406.

20 J. P. Perdew, K. Burke and M. Ernzerhof, *Phys. Rev. Lett.*, 1996, **77**, 3865–3868.

21 L. Desgranges, G. Baldinozzi, G. Rousseau, J.-C. Nièpce and G. Calvarin, *Inorg. Chem.*, 2009, **48**, 7585–92.

22 P. C. Debets, *Acta Crystallogr.*, 1966, **21**, 589–593.

23 B. O. Loopstra, *Acta Crystallogr.*, 1964, **17**, 651–654.

24 D. A. Andersson, F. J. Espinosa-Faller, B. P. Uberuaga and S. D. Conradson, *J. Chem. Phys.*, 2012, **136**, 234702.

25 M. Methfessel and A. T. Paxton, *Phys. Rev. B*, 1989, **40**, 3616–3621.

26 B. Dorado, B. Amadon, M. Freyss and M. Bertolus, *Phys. Rev. B*, 2009, **79**, 235125.

27 P. C. Burns, R. C. Ewing and F. C. Hawthorne, *Can. Mineral.*, 1997, **35**, 1551–1570.

28 W. . Zachariasen, *J. Less Common Met.*, 1978, **62**, 1–7.